ORGANOMETALLICS®

Volume 12, Number 11, November 1993

Communications

Complex Rearrangements of Polysilylacylsilanes from Treatment with $TiCl_4$

A. G. Brook,* Michael Hesse, Kim M. Baines, Rajkumar Kumarathasan, and Alan J. Lough

Lash Miller Chemical Laboratories, University of Toronto, Toronto M5S 1A1, Ontario, Canada

Received May 26, 1993®

Summary: Treatment of polysilylacylsilanes $(Me_3Si)_3SiCOR$ (R = t-Bu, Ad, 2,2,2-bicyclooctyl (=BCO)) with 1 equiv of $TiCl_4$ in the cold yields 1,3-bis(silanols) Me_3Si–SiMeOH–C($SiMe_3$)R–$SiMe_2OH$ on aqueous workup, as shown by crystal structures of the BCO and tert-butyl derivatives. A mechanism involving the 1,2-migrations of silyl groups to adjacent carbocationic centers and of alkyl groups to silicenium ion centers is proposed to account for the features of the rearrangement.

In the course of another investigation we were led to treat one of our polysilylacylsilanes, $(Me_3Si)_3SiCO(t\text{-Bu})$ (**1a**), overnight with 1 equiv of titanium tetrachloride in methylene chloride at −20 °C. The solution immediately became strongly orange-brown, and after this solution stood overnight in the cold without apparent change, aqueous workup gave the single colorless crystalline product **2a** in quantitative yield. Structures based on the NMR data were difficult to reconcile with other data (e.g. mass spectroscopy), and it was not immediately clear whether the compound was the diol **2a** or its anhydro derivative **3a**, a disilaoxetane, which might be easily formed from **2a** (see eq 1). Similar behavior was exhibited by both the adamantyl acylsilane **1b** and the 2,2,2-bicyclooctyl acylsilane **1c**. Ultimately the structures of the reaction products were established as the 1,3-bis(silanols) **2** on the basis of the crystal structure of **2c**, whose ORTEP[1] diagram is shown in Figure 1. No evidence for the second possible diastereomer in any of the examples was found. It is

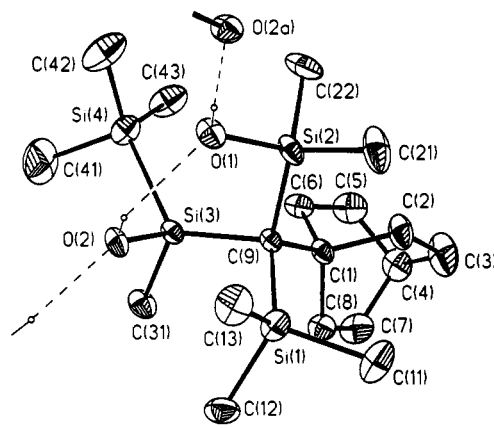

Figure 1. View of the molecule **2c**, Me_3Si–SiMeOH–C(Me_3-Si)C_8H_{13}–$SiMe_2OH$, showing the atomic labeling scheme. Thermal ellipsoids are at the 25% probability level.

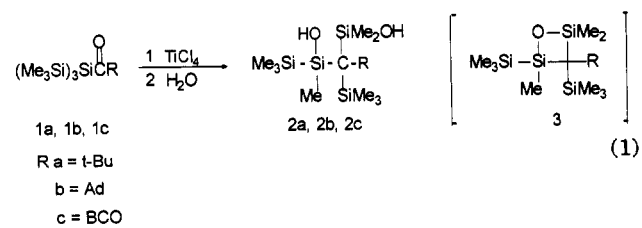

(1)

obvious that dramatic structural rearrangements have occurred during the formation of **2** from **1**.

The NMR and other spectroscopic data given in ref 2 for compounds **2a**, **2b**, and **2c** are remarkably similar and wholly consistent with the established structures. In each

* Abstract published in *Advance ACS Abstracts*, October 1, 1993.

(1) Johnson, C. K. ORTEPII; Report ORNL-5138; Oak Ridge National Laboratory: Oak Ridge, TN, 1976.

0276-7333/93/2312-4259$04.00/0

Scheme I

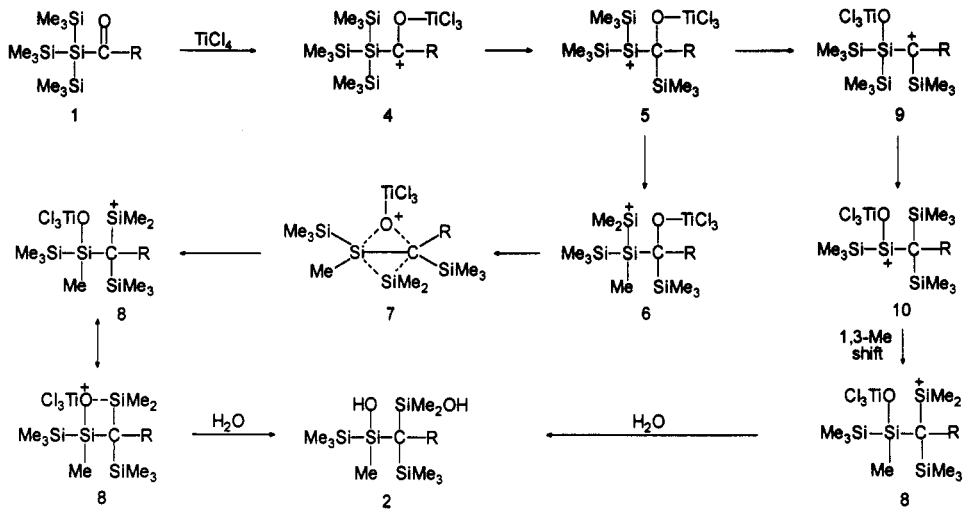

case, however, the mass spectrum indicated that the highest ion mass present was $M^+ - H_2O$, and the OH stretching absorption in the infrared spectrum was rather weak, which initially suggested the structure **3** for the reaction products. However, the high-quality crystal structure of **2c** and the ^1H NMR data for **2a** clearly established the presence of the SiOH groups.[3]

In an attempt to provide a mechanism for the conversion of **1** to **2**, some details of the rearrangements are easily recognized. Thus, in a comparison of the structure of the product with that of the starting material, it is obvious that a 1,2-migration of oxygen from carbon to silicon, a 1,2-migration of a trimethylsilyl group from silicon to carbon, and migration of a methyl group from one silicon atom to another have occurred. Scheme I provides two possible pathways for the overall rearrangement.

Coordination of titanium tetrachloride with the carbonyl oxygen would be expected to form the carbocation **4**, to which site a trimethylsilyl group could be expected to migrate,[4] yielding the silicenium ion **5**. Methyl migration from silicon to an adjacent cationic site localized on silicon (**5** → **6**) is well-known.[5] Less certain is the manner by which the oxygen, initially on carbon, and the dimethylsilyl group on silicon exchange locations (**6** → **8**), and in the absence of factual knowledge at this time, we suggest as one possibility the exchange (either concerted or stepwise) through the intermediate **7**, leading through **8** to the observed product **2** on hydrolytic workup. Alternatively, the oxygen in **5** could migrate to the silicenium site to give

Table I. Summary of Crystal Data, Details of Intensity Collection, and Least-Squares Refinement Parameters

empirical formula	$C_{18}H_{42}O_2Si_4$
M_r	402.9
cryst size, mm	0.4 × 0.15 × 0.15
cryst class	monoclinic
space group	$P2_1/n$
a, Å	11.325(2)
b, Å	9.496(2)
c, Å	22.726(5)
β, deg	101.32(3)
V, Å^3	2396.4(8)
Z	4
D_{calc}, g cm^{-3}	1.12
μ(Mo Kα), cm^{-1}	2.57
F(000)	888
ω scan width, deg	0.5 + 0.63 tan θ
range θ collected, deg	2–26
indices collected	h, −11 to 0; k, −13 to +13; l, −27 to +27
total no. of rflns	10 052
no. of unique rflns	4677
R_{int}	0.032
no. of obsd data ($F > 6\sigma(F)$)	2333
min/max transmissn coeff	0.616/0.710
R	0.052
R_w	0.067
goodness of fit	0.99
largest/mean Δ/σ	0.02/0.00
no. of params refined	226
max/min density in ΔF map, e Å^{-3}	+0.81/−0.19

(2) Physical properties of **2a** are as follows. Mp: 141 °C (from C_6H_6). Anal. Calcd for $C_{14}H_{38}O_2Si_4$: C, 47.93; H, 10.92. Found: C, 48.37; H, 10.73. ^1H NMR ($CDCl_3$): δ 0.15 (9H, s, Me_3Si), 0.30 (3H, s, Me_3Si), 0.39, 0.40 (each 3H, s, diastereotopic Me_2Si; in C_6D_6 these signals became one 6H signal at 0.39 ppm), 0.52 (3H, s, MeSi), 1.20 (9H, s, Me_3C), 1.6, 1.9 (each 1H, s, OH in the non-H-bonding case;[3] in the intramolecular H-bonded case an approximately 2H broad signal occurred between 1.5 and 2.05 ppm). ^{13}C NMR ($CDCl_3$): δ 0.17 (Me_3Si–Si), 6.57 (Me_3Si–C), 5.93, 6.72, 8.05 (Me–Si), 34.00 (Me_3C), 34.98 (Me_3C). ^{29}Si NMR ($CHCl_3$): δ −17.68 (Me_3Si–Si), −1.24 (Me_3Si–C), 15.38 (Me_2Si), 15.62 (Me–Si). The ^{29}Si–^1H shift correlated spectra showed that the Si peak at −1.24 ppm correlated with the 9H Me_3Si peak at 0.30 (i.e. Me_3Si–C), the 15.38 ppm Si peak correlated with both 3H Me signals at 0.39 and 0.40 (i.e. $SiMe_2$), the 15.62 ppm Si peak correlated with the 3H signal at 0.52 ppm (i.e. Me–Si), and the −17.68 ppm Si peak correlated with the 9H Me_3Si signal at 0.15 (i.e. Me_3Si–Si). HR-MS: calcd for $M^+ - H_2O$ 332.1843, found 332.1847. MS (m/e(%)): 332 (23, $M^+ - H_2O$), 317 (100, $M^+ - H_2O$ – Me), 259 (90, $M^+ - H_2O$ – Me_3Si), 171, 147, 131, 73 (100, Me_3Si^+). IR (CCl_4): 3676 cm^{-1} (OH, weak). Physical properties of **2b** are as follows. Mp: 189–191 °C after 6 h reflux in benzene and then recrystallization. Anal. Calcd for $C_{20}H_{44}O_2Si_4$: C, 55.99; H, 10.33. Found: C, 56.11; H, 10.11. ^1H NMR (C_6D_6): δ 0.23 (9H, s, Me_3Si–Si), 0.45, 0.46 (each 3H, s, diastereotopic Me_2Si), 0.49 (9H, s, Me_3Si–C), 0.58 (3H, s, Me–Si), 1.5–2.04 (>17H, m, Ad + 2 OH). ^{13}C NMR (C_6D_6): δ 0.56 (Me_3Si), 7.56 (Me_3Si, broad), 6.90, 7.57, 9.05 (Me–Si), 29.98 (Ad CH), 36.82, 44.67 (br) (Ad CH_2), 44.68 (Ad quat C). ^{29}Si NMR: δ (C_6D_6) −16.32 (Me_3Si–Si), −0.57 (Me_3Si–C), 14.78 (MeSiOH), 14.96 (Me_2SiOH). HR-MS: calcd for $C_{20}H_{44}O_2Si_4$ ($M^+ - H_2O$) 410.2313, found 410.2314. MS (m/e (%)): 410 (40, $M^+ - H_2O$), 395 (28, $M^+ - H_2O$ – Me), 337 (100, $M^+ - H_2O$ – Me_3Si). Physical properties of **2c** are as follows. Mp: 191–193 °C (from C_6H_6). ^1H NMR (C_6D_6): δ 0.21, 0.41 (each 9H, s, Me_3Si), 0.42, 0.43 (each 3H, s, diastereotopic Me_2Si), 0.52 (3H, s, MeSi), 1.38–1.50, 1.72–1.92 (6CH_2 + CH + 2OH). ^{13}C NMR ($CDCl_3$): δ 0.37 (Me_3Si–Si), 6.54, 7.40, 8.66 (each Me–Si), 7.06 (Me_3Si–C), 23.60 (CH), 27.06, 32.92 (CH_2), 35.71, 35.98 (quat C). ^{29}Si NMR (C_6H_6): δ −15.76 (Me_3Si–Si), −1.15 (Me_3Si–C), 14.83, 15.09 (Me_2Si and MeSi). IR (CCl_4): 3100–3600 (broad, weak). HR-MS: calcd for $C_{18}H_{40}OSi_4$ ($M^+ - H_2O$) 384.2156, found 384.2151.

(3) Two forms of **2a** appear to have been isolated. The sample used in the X-ray analysis showed the two OH groups in the ^1H NMR spectrum as a very broad 2H signal. If this material was refluxed in benzene and the solution then cooled quickly, the ^1H NMR spectrum showed two distinct 1H signals at 1.6 and 1.9 ppm.

(4) Kumada, M.; Nakajima, J.; Ishikawa, M.; Yamamoto, Y. *J. Org. Chem.* **1958**, *23*, 292.

(5) Whitmore, F. C.; Sommer, L. H.; Gould, J. R. *J. Am. Chem. Soc.* **1947**, *69*, 1976.

Table II. Bond Lengths (Å)

Si(1)–C(9)	1.947(4)	Si(1)–C(11)	1.886(5)
Si(1)–C(12)	1.868(5)	Si(1)–C(13)	1.884(5)
Si(2)–O(1)	1.649(3)	Si(2)–C(9)	1.903(4)
Si(2)–C(21)	1.871(6)	Si(2)–C(22)	1.872(6)
Si(3)–Si(4)	2.380(2)	Si(3)–O(2)	1.667(4)
Si(3)–C(9)	1.934(3)	Si(3)–C(31)	1.875(4)
Si(4)–C(41)	1.862(7)	Si(4)–C(42)	1.840(6)
Si(4)–C(43)	1.864(6)	C(1)–C(2)	1.547(6)
C(1)–C(6)	1.535(6)	C(1)–C(8)	1.545(6)
C(1)–C(9)	1.608(5)	C(2)–C(3)	1.538(7)
C(3)–C(4)	1.505(9)	C(4)–C(5)	1.505(7)
C(4)–C(7)	1.526(8)	C(5)–C(6)	1.534(7)
C(7)–C(8)	1.539(7)	O(1)–H(01)	0.64(4)
O(2)–H(02)	0.66(5)	O(1)···O(2)	2.727(8)
O(1)···O(2A)	2.732(8)	H(10)···O(2A)	2.09(5)
H(20)···O(1)	2.18(5)		

carbocation **9**, followed by a second trimethylsilyl migration leading to the new, oxygen-stabilized silicenium ion **10**. If a 1,3-methyl shift from sp^3- to sp^2-hybridized silicon were to occur (a process observed previously by Eaborn,[6] Wiberg,[7] and ourselves[8]), the ion **8** would again be formed prior to the hydrolytic workup. We plan to investigate further the scope of this new rearrangement of polysilylacylsilanes, in the course of which we hope to establish more completely the details of the mechanism.

X-ray Structural Determination. Compound **2c** formed small needles from C_6H_6 which were air-stable. Intensity data were collected on an Enraf-Nonius CAD-4 diffractometer at room temperature, using graphite-monochromated Mo Kα radiation (λ = 0.710 73 Å). The ω-scan technique was applied using variable scan speeds (1.65–16.48°/min in ω). The intensities of three standard reflections measured every 2 h showed no decay. Data were corrected for Lorentz and polarization effects, and a semiempirical absorption correction was applied. The structure was solved by direct methods. Non-hydrogen atoms were refined anisotropically by least squares to minimize $\sum(F_o - F_c)^2$. Hydrogen atoms were positioned on geometric grounds and included in the refinement as riding atoms (C–H = 0.96 Å, U_{iso} = 0.107(3) Å^2). The hydroxyl hydrogen atoms were located from a difference Fourier map and were refined with isotropic thermal parameters. There were no chemically significant features in the final difference Fourier map.

The structure of **2c** contains weak intramolecular and intermolecular O–H···O interactions. The molecules form infinite chains (through 2_1 screw axes) via the intermolecular O(1)–H(O1)–O(2A) interactions (O(1)···O(2A) = 2.732(8) Å). The intramolecular O(2)–H(O2)–O(1) interactions (O(1)···O(2) = 2.727(8) Å) may have a role in controlling the conformation of the molecule. Crystal data, data collection, and least-squares parameters are listed in Table I. The bond lengths and bond angles observed are listed in Tables II and III. All calculations and graphics were performed using SHELXTL PC[9] on a 486-33 personal computer. Atomic coordinates and other data concerning the crystal structures are given in the supplementary material.

Table III. Bond Angles (deg)

C(9)–Si(1)–C(11)	113.8(2)	C(9)–Si(1)–C(12)	114.3(2)
C(11)–Si(1)–C(12)	105.8(2)	C(9)–Si(1)–C(13)	114.5(2)
C(11)–Si(1)–C(13)	103.4(2)	C(12)–Si(1)–C(13)	103.8(2)
O(1)–Si(2)–C(9)	103.5(2)	O(1)–Si(2)–C(21)	108.7(2)
C(9)–Si(2)–C(21)	116.2(2)	O(1)–Si(2)–C(22)	105.7(2)
C(9)–Si(2)–C(22)	116.5(2)	C(21)–Si(2)–C(22)	105.5(2)
Si(4)–Si(3)–O(2)	101.7(1)	Si(4)–Si(3)–C(9)	124.6(1)
O(2)–Si(3)–C(9)	106.1(2)	Si(4)–Si(3)–C(31)	102.8(2)
O(2)–Si(3)–C(31)	102.5(2)	C(9)–Si(3)–C(31)	116.2(2)
Si(3)–Si(4)–C(41)	102.7(2)	Si(3)–Si(4)–C(42)	113.6(2)
C(41)–Si(4)–C(42)	104.5(3)	Si(3)–Si(4)–C(43)	118.7(2)
C(41)–Si(4)–C(43)	104.9(3)	C(42)–Si(4)–C(43)	110.6(3)
C(2)–C(1)–C(6)	106.6(3)	C(2)–C(1)–C(8)	107.1(3)
C(6)–C(1)–C(8)	106.0(3)	C(2)–C(1)–C(9)	112.5(3)
C(6)–C(1)–C(9)	111.0(3)	C(8)–C(1)–C(9)	113.2(3)
C(1)–C(2)–C(3)	110.0(4)	C(2)–C(3)–C(4)	110.4(4)
C(3)–C(4)–C(5)	109.7(4)	C(3)–C(4)–C(7)	107.6(5)
C(5)–C(4)–C(7)	107.8(4)	C(4)–C(5)–C(6)	110.1(4)
C(1)–C(6)–C(5)	111.1(3)	C(4)–C(7)–C(8)	109.3(4)
C(1)–C(8)–C(7)	111.2(4)	Si(1)–C(9)–Si(2)	106.2(2)
Si(1)–C(9)–Si(3)	106.7(2)	Si(2)–C(9)–Si(3)	104.9(2)
Si(1)–C(9)–C(1)	113.1(2)	Si(2)–C(9)–C(1)	113.6(2)
Si(3)–C(9)–C(1)	111.7(2)	H(10)–O(1)–Si(2)	114(4)
H(20)–O(2)–Si(3)	112(4)	O(2A)···H(10)–O(1)	173(5)
O(2)–H(20)···O(1)	142(5)		

A crystal structure for **2a** was also obtained but was of poor quality, partly because of the crystals, which were probably twinned. However, it did clearly show that the atomic connectivities of the skeleton of **2a** were the same as those found in compound **2c**.

Acknowledgment. This research was supported by the Natural Science and Engineering Council of Canada.

Supplementary Material Available: Tables of atomic coordinates, anisotropic thermal parameters, hydrogen atom coordinates, and crystal data and data collection and refinement details (6 pages). Ordering information is given on any current masthead page.

OM9303562

(6) Eaborn, C.; Happer, D. A.; Hitchcock, P. B.; Hopper, S. P.; Safa, K. D.; Washburne, S. S.; Walton, D. M. *J. Organomet. Chem.* **1980**, *186*, 309.

(7) Wiberg, N.; Wagner, G. *Chem. Ber.* **1986**, *119*, 1467.

(8) Baines, K. M.; Brook, A. G.; Ford, R. R.; Lickiss, P. D.; Saxena, A. K.; Chatterton, W. J.; Sawyer, J. F.; Behnam, B. A. *Organometallics* **1989**, *8*, 693.

(9) Sheldrick, G. M. SHELXTL PC; Siemens Analytical X-Ray Instruments, Inc., Madison, WI, 1989.